

Electrochemical characterization of metastable pitting of 3003 aluminum alloy in ethylene glycol–water solution

Lin Niu · Y. Frank Cheng

Received: 5 January 2007 / Accepted: 9 May 2007 / Published online: 10 July 2007
© Springer Science+Business Media, LLC 2007

Abstract The corrosion and electrochemical behavior of 3003 aluminum alloy in ethylene glycol–water solution were investigated by electrochemical techniques. It is found that the oxide film formed on aluminum depends on the dissolved oxygen in the solution. In the presence of oxygen, a layer of aluminum oxide film forms on the aluminum surface to protect the substrate from corrosion. In the absence of oxygen, the film formed is mainly aluminum-alcohol film that is less compact and less resistant to corrosion. The aluminum oxide film and aluminum-alcohol film have the different susceptibilities to chloride ion attack for pit initiation. There is a higher pitting susceptibility for aluminum oxide-covered electrode. The increase in temperature decreases the resistance of aluminum electrode to corrosion reaction. However, the resistance to pitting corrosion increases.

Introduction

Aluminum alloys, due to their favorable strength-to-weight and corrosion resistance properties, have been widely used in a variety of industry fields, including the automotive industry. In particular, aluminum alloys have been broadly

integrated into vehicular heat exchange systems, replacing more traditional materials like stainless steels and copper alloys. However, aluminum alloys are prone to corrosion even in fully inhibited coolants [1].

It has been commonly accepted that the corrosion resistance of aluminum alloys is mainly due to an oxide layer formation [2, 3]. Corrosion of aluminum materials is usually manifested by random generation of pits that are associated with the presence of halide ions, such as chloride ions, which are the most frequently encountered species in service, including automotive coolant [4, 5]. The pitting corrosion of aluminum and aluminum alloys has been studied extensively in the various aqueous solutions, and theories and models have been developed to illustrate the pit initiation, growth and repassivation processes [2]. However, there has been few work performed in automotive coolant such as ethylene glycol. Wong et al. [6] investigated the corrosion characteristics of some aluminum alloys in ethylene glycol/water solutions under conditions relevant to the operation of aluminum solar heat collector systems, and found that the corrosion resistance of aluminum alloys in the test solutions was marginally acceptable. In the presence of common water contaminants, such as chloride ions, severe pitting corrosion was observed. However, the work did not touch the mechanistic aspects of the electrochemical reactions occurring on aluminum electrode, and did not reveal the mechanism of pitting corrosion of aluminum alloys, either.

This work was to study the fundamentals of corrosion and electrochemical behavior of 3003 aluminum alloy in chloride-containing ethylene glycol–water solution by measurements of corrosion potential, electrochemical impedance spectroscopy (EIS) and potentiodynamic polarization curves. The mechanism of pitting corrosion of aluminum alloy was analyzed. The effects of dissolved

L. Niu
School of Chemistry and Chemical Engineering, Shandong
University, Jinan, Shandong 250100, China

Y. F. Cheng (✉)
Department of Mechanical and Manufacturing Engineering,
University of Calgary, 2500 University Avenue NW, Calgary,
AB, Canada T2N 1N4
e-mail: fcheng@ucalgary.ca

oxygen and temperature on aluminum pitting corrosion were discussed.

Experimental procedure

The working electrode for electrochemical tests was made of 3003 aluminum alloy with the chemical composition (wt, %): Cu 0.20, Fe, 0.70, Si 0.60, Mn 1.50, Mg 0.05, Cr 0.05, Zn 0.10, Ti 0.05, and Al balance. The specimen was ground with 600 grit emery paper on all faces. The unexposed edges were coated with a masking paint to prevent crevice corrosion between the epoxy mount and the electrode. The specimens were embedded in epoxy resin leaving a working area of 0.326 cm². The working surface was ground with 1000 grit emery paper and subsequently polished with 15, 9, 3 and 1 μm alumina powder pastes, cleaned by distilled water and methanol.

The test solution was a 50% ethylene glycol + 50% distilled water + 100 ppm Cl⁻ solution to simulate the automotive coolant. The solution was made from analytic grade reagents and ultra-pure water (18 MΩ). To investigate the effect of dissolved oxygen on the aluminum corrosion, tests were performed open to air unless it was stated that the solution was purged with high-purity (99.999%) nitrogen gas. The test temperature was maintained through a water bath controlled by a thermoelectric couple (± 0.1 °C).

The EIS measurements were performed on a three-electrode system through a Solartron 1280Z Electrochemical Interface. 3003 aluminum alloy was used as working electrode, saturated calomel electrode (SCE) as reference electrode and a platinum plate as counter electrode. In the polarization curve measurements, the potential sweep rate was 1 mV/s. In EIS measurements, the measuring frequency ranges were varied from 20,000 Hz to 0.01 Hz, and the AC signal amplitude was 5 mV. All the EIS measurements were conducted at open-circuit potential.

Results

Corrosion potential measurements

Figure 1 shows the corrosion potential as a function of immersion time in the aerated test solution. It is seen that corrosion potential of the electrode increased rapidly from -0.75 V to about -0.55 V within 2,000 s. After that, the corrosion potential fluctuated around -0.55 V with the immersion time.

Figure 2 shows the corrosion potential as a function of time in the deaerated test solution. It is seen that, different from that in the aerated solution, corrosion potential of the electrode kept increasing until 18,000 s of immersion and

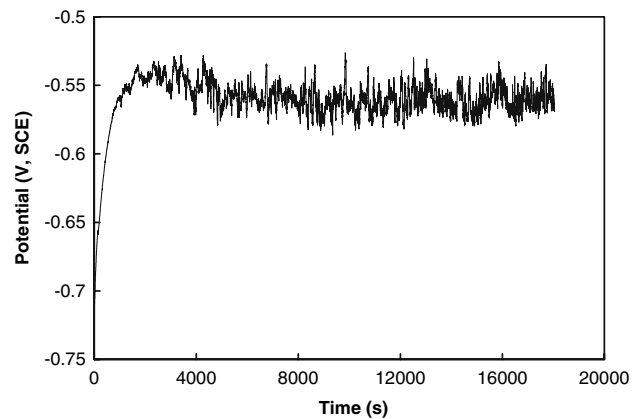


Fig. 1 The corrosion potential as a function of immersion time in the aerated test solution

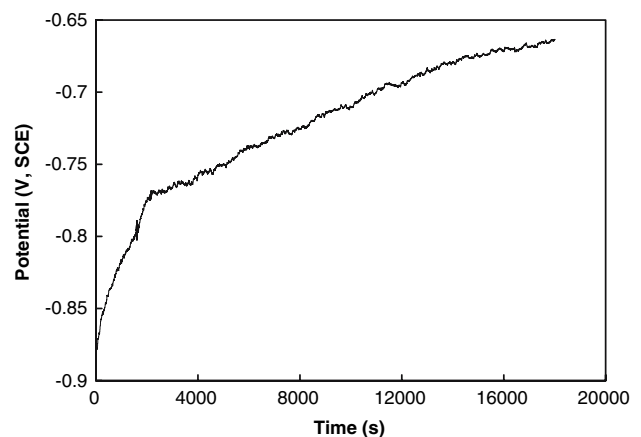


Fig. 2 The corrosion potential as a function of immersion time in the deaerated test solution

an approximately steady-state value was not reached. Furthermore, the potential values were more negative in deaerated solution than those in aerated solution over the whole testing time range. Moreover, the potential fluctuation was much smaller in the deaerated solution.

Electrochemical impedance spectroscopy and polarization curve measurements

Figure 3 shows the EIS plots of 3003 aluminum electrode at 60 s and 1,800 s of immersion in the aerated solution, respectively. It is seen that both impedance spectra showed the same feature, i.e., a depressed semicircle in the high-frequency range and a straight line with the slope of approximately 45° (not exactly 45°) at the low frequency range. With the increase of immersion time, the diameter of the high-frequency semicircle increased significantly.

Figure 4 shows the polarization curves of 3003 aluminum electrode in the aerated and deaerated solutions at

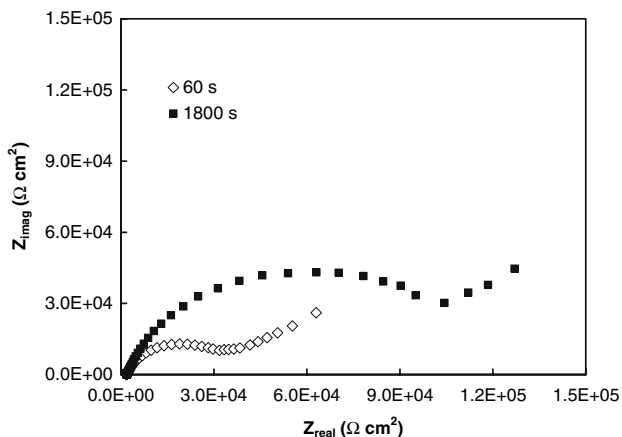


Fig. 3 EIS plots of 3003 Al electrode in the aerated test solution at 60 s and 1,800 s of immersion, respectively

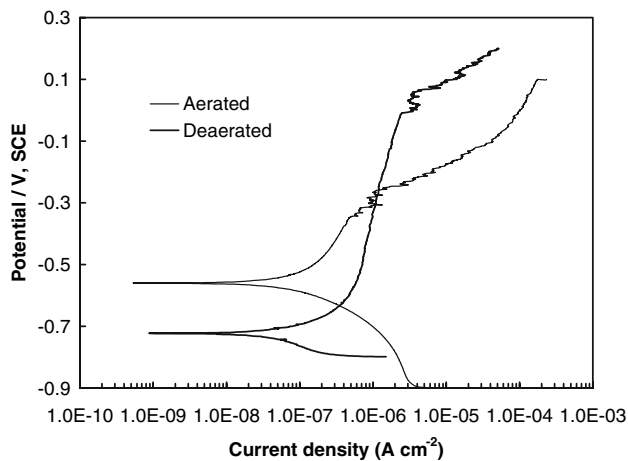


Fig. 4 The polarization curves of 3003 Al electrode after 18,000 s of immersion in the aerated and deaerated test solutions

18,000 s of immersion. It is seen that, with a higher corrosion potential, the electrode experienced a lower passive current density and a much narrower passive potential range in the aerated solution. There was a much wider passive range and a higher pitting onset potential for aluminum electrode in the deaerated solution than in the aerated solution.

Figure 5 shows the EIS plots of the aluminum electrode after 60 s of immersion in the aerated test solution under temperatures of 20, 30, 40 and 50 °C, respectively. All the impedance spectra showed the same characteristic as the previously measured ones, i.e., a depressed semicircle in the high-frequency range and a straight line with an approximate 45° slope in the low-frequency range. Furthermore, the size of the semicircle decreased with the increasing temperature.

Figure 6 shows the polarization curves of aluminum electrode in the aerated solution at the various tempera-

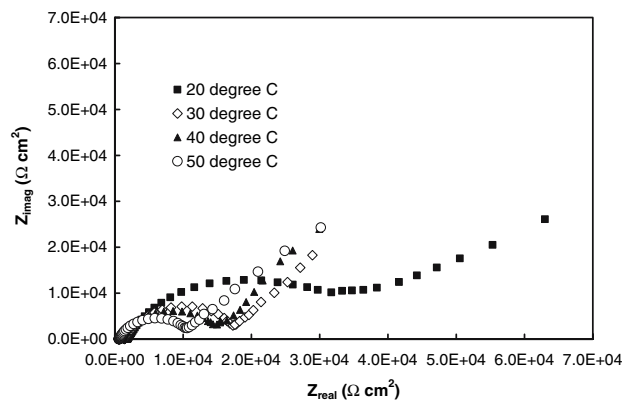


Fig. 5 The EIS plots of 3003 Al electrode after 60 s of immersion in the aerated test solution at 20, 30, 40 and 50 °C, respectively

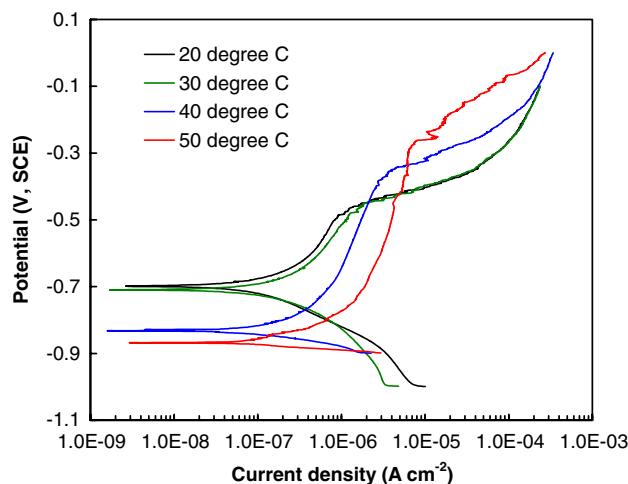


Fig. 6 The polarization curves of 3003 Al electrode in the aerated test solution at 20, 30, 40 and 50 °C, respectively

tures. It is seen that, with the increase in temperature, the corrosion potential of aluminum decreased and the anodic dissolution current increased. Furthermore, the increasing temperature resulted in the increase of the pitting onset potential.

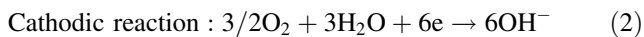
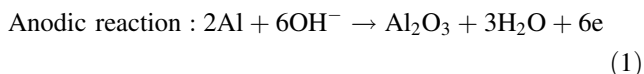
Discussion

Oxidation of aluminum alloy in ethylene glycol–water solution

It has been acknowledged [2, 3] that the excellent corrosion resistance of aluminum alloys is attributed to the formation of a layer of oxide film. The positive increase of corrosion potential of 3003 aluminum electrode upon immersion in both aerated (Fig. 1) and deaerated (Fig. 2) solutions shows that the electrode is oxidized upon the immersion in the solutions. The different time dependences of corrosion

potential indicate the different film-formation reactions occurring on aluminum electrode in the presence and absence of oxygen.

The aluminum oxidation in the presence of oxygen is characterized by:

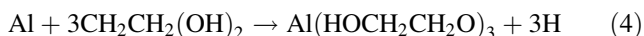


The dissolved oxygen diffuses towards the aluminum electrode surface, and the reduction reaction generates hydroxide ions that are used by the oxidation of aluminum to form aluminum oxide, resulting in the increase of corrosion potential of the electrode immediately immersed in the solution. The further growth of oxide film occurs at the aluminum/oxide interface and depends on the diffusion of oxygen through the oxide film. The generated hydroxide ions self-catalyze the film-formation reaction, accompanying the aluminum dissolution. After the film formation and dissolution achieves an equilibrium-status, corrosion potential of the electrode reaches a relatively steady-state value. Since the test solution is open to air, the oxygen supplement is sufficient to support the film formation, resulting in the rapid, positive increase of corrosion potential towards the steady-state value, as shown in Fig. 1. Moreover, the growth of the aluminum oxide film results in the thicker and the more compact oxide film with the higher resistance to corrosion. Therefore, the measured film resistance at 1,800 s of immersion is much higher than that at 60 s of immersion (Fig. 3). Furthermore, the reaction at the aluminum/oxide interface is dominated by diffusion process, as indicated by the straight line with an approximately 45° slope in the low-frequency range of EIS plots, of oxygen through the oxide film (not the pure diffusion-controlled electrode process since the slope is not exactly 45°).

In the absence of oxygen, the increasing corrosion potential of the aluminum electrode upon immersion in the solution (Fig. 2) indicates that aluminum is also experiencing oxidation, and a layer of film is being formed on the electrode surface. The cathodic reaction is dominated by the reduction of ethylene glycol:



Therefore, aluminum is oxidized by ethylene glycol:



Apparently, the formation of aluminum-ethylene glycol film depends on the ionic bonding of ethylene glycol to

aluminum by losing the protons from both OH groups. The further growth of the film is speculated to be the formation of a hydrophobic network of hydrocarbon “tails” which extend to the solution and hinder the access of water molecules to the surface [7]. A steady-state value cannot be achieved even after 18,000 s of immersion in this work.

It has been established [8] that, without defects and pits, the metal oxide film is much more compact and thus more resistant to corrosion than metal-alcohol film. In addition, the current work shows that corrosion potential of aluminum reaches a more positive steady-state value more rapidly in aerated solution than in deaerated solution. Therefore, the cathodic reaction is dominated by the oxygen reduction in aerated solution even though ethylene glycol exists in the solution.

Metastable pitting of 3003 aluminum alloy in ethylene glycol–water solution

Metastable pitting process of metals includes initiation, growth and repassivation of metastable pits. Generally, the time dependence of corrosion potential could reflect the variation of electrode surface state and nature with time. As shown in Fig. 1, after 1,800 s of immersion, corrosion potential of aluminum electrode achieves a relatively steady-state value, indicating the formation of a layer of oxide film on the electrode surface. The frequent potential oscillations around a steady-state potential value could be attributed to the metastable pitting processes. Similar phenomena were observed in 2024 T3 aluminum alloys, which undergo pitting corrosion in aerated chloride solutions [3].

It has been established [9] that the spontaneous potential and/or current fluctuations for metals or alloys in chloride-containing solutions indicate the initiation, growth and repassivation of metastable pits. Furthermore, each typical potential or current noise signal corresponds to one metastable pit [10]. Apparently, the metastable pits could be initiated on aluminum alloy in the chloride-containing ethylene glycol–water solution under open-circuit potential, under which the aluminum electrode is in free-corrosion status. However, the transition of metastable pits toward stability is restricted under free-corrosion condition since no phenomenon relevant to stable pitting has been observed in this work, such as a continuous, negative shift of the electrode potential. Author’s previous work [11] has established that a pit stabilization criterion, the ratio of the pit dissolution current to pit radius, has to be met to enable the transition of metastable pits to stable pits. This criterion reflects the difference of the cation concentrations between the bulk solution and the pit electrolyte. Without the further enhancement of the solution aggressiveness, such as an increase in chloride concentrations or an enhanced anodic

polarization, the aluminum pitting under the test condition will be remained to be metastable.

The current work shows that the aluminum-alcohol film is less susceptible to pitting than Al_2O_3 film, as indicated by the less frequent, smaller potential fluctuations (Fig. 2) and a wider passivity range as well as a higher pitting onset potential (Fig. 4). This phenomenon is attributed to the different composition and structure of the films formed in the presence and absence of oxygen and the different susceptibilities of the films to chloride ion attack for pit initiation. According to point defect model [12] and the previous work on carbon steel pitting [13], the role of chloride ions in pit initiation is to absorb and occupy the oxygen vacancies in the oxide film at oxide/solution interface, resulting in the generation of cation vacancies that diffuse through the film and accumulate at the metal/oxide interface to cause the local thinning of the film or detachment from the metal. Like iron oxide, Al_2O_3 has the cubic crystalline structure with an octahedral coordination geometry [14]. It is assumed that the initiation of metastable pits on aluminum electrode is due to the replacement of oxygen vacancies with chloride ions, generating cation vacancies at oxide/solution interface.

To date, there has been limited knowledge on the structure of metal-alcohol film. The current work shows that the film is relatively insensitive to chloride ion attack, indicating that the film grows with a different mechanism from metal oxide film. Furthermore, the interactions between C–O bond and O–Al bond and their strength could affect the stability of oxygen species and the absorption of chloride ions on the film. The further characterization of the structure and properties of the aluminum-alcohol film is essential to reveal the corrosion and electrochemical behavior of aluminum in ethylene glycol–water solution in the absence of oxygen.

Effect of temperature on pitting of aluminum alloy

Generally, the increase in temperature is favorable for the various interfacial reaction processes. Furthermore, as the temperature of solution goes up, the concentration of dissolved oxygen decreases. The decreased oxygen amount in the solution and the enhanced aluminum dissolution result in the thinner and/or less compact aluminum oxide film on the electrode surface. The resistance of the film decreases with the increasing temperature, as shown in Fig. 5. Moreover, the decreasing oxygen amount in the solution at

high temperature causes the film-formation to be favorable for aluminum-alcohol film, at least in quantity. Although the anodic dissolution current increases, the film becomes less susceptible to pitting due to the alternation of the film composition at high temperature, as indicated by the increasing pitting onset potential in Fig. 6.

Conclusions

The composition of the oxide film formed on aluminum electrode in ethylene glycol–water solution depends on the existence of dissolved oxygen. In the presence of oxygen, a layer of aluminum oxide film forms on the aluminum surface to protect the substrate from corrosion. In the absence of oxygen, the film formed is mainly aluminum-alcohol film that is less compact and less resistant to corrosion.

The aluminum oxide film and aluminum-alcohol film have the different susceptibilities to chloride ion attack for pit initiation. There is a higher pitting susceptibility for aluminum oxide-covered electrode.

The increase in temperature decreases the resistance of aluminum oxide film to corrosion reaction. However, the resistance to pitting corrosion increases.

Acknowledgements This work was supported by Canada Research Chairs Program and Natural Science and Engineering Research Council of Canada (NSERC).

References

1. Miller WS, Zhuang L, Bottema J, Wittebrood AJ, De Smet P, Haszler A, Vierendege A (2000) *Mat Sci Eng A* 280:37
2. Szklarska-Smialowska Z (1999) *Corros Sci* 41:1743
3. Frankel GS (1998) *J Electrochem Soc* 145:2186
4. De Micheli SM (1978) *Corros Sci* 18:605
5. Baumgärtner M, Haesche H (1990) *Corros Sci* 31:231
6. Wong D, Swette L, Cocks FH (1979) *J Electrochem Soc* 126:11
7. Shu QQ, Love PJ, Bayman A, Hansma PK (1982) *Appl Surf Sci* 13:374
8. Cheng YF (2005) *B Electrochem* 21:503
9. Szklarska-Smialowska Z (1986) In: *Pitting of metals*, NACE, Houston, TX, p 347
10. Cheng YF, Luo JL (1999) *J Electrochem Soc* 146:970
11. Cheng YF, Wilmott M, Luo JL (1999) *Br Corros J* 34:280
12. Macdonald DD (1992) *J Electrochem Soc* 139:3434
13. Cheng YF, Luo JL (1999) *Electrochimica Acta* 44:2947
14. Callister WD (2003) In: *Materials science and engineering: an introduction*, John Wiley & Sons, New York, p 247